Molecular Biology of the Cell
Vol. 16, 5400–5409, November 2005

# *Drosophila* Nod Protein Binds Preferentially to the Plus Ends of Microtubules and Promotes Microtubule Polymerization In Vitro[D]

**Wei Cui,*†‡ Lisa R. Sproul,‡§ Susan M. Gustafson,* Heinrich J.G. Matthies,‖ Susan P. Gilbert,§ and R. S. Hawley*¶**

*Stowers Institute for Medical Research, Kansas City, MO 64110; †Department of Pathology and Clinical Laboratory, University of Kansas Medical Center, Kansas City, KS 66160; §Department of Biological Sciences, University of Pittsburgh, Pittsburgh, PA 15260; ‖Department of Biological Sciences, Vanderbilt University, Nashville, TN 37235; and ¶Department of Molecular Biosciences, University of Kansas, Lawrence, KS 66045

Submitted June 29, 2005; Revised August 12, 2005; Accepted August 25, 2005
Monitoring Editor: J. Richard McIntosh

**Nod, a nonmotile kinesinlike protein, plays a critical role in segregating achiasmate chromosomes during female meiosis. In addition to localizing to oocyte chromosomes, we show that functional full-length Nod-GFP ($Nod_{FL}$-GFP) localizes to the posterior pole of the oocyte at stages 9–10A, as does kinesin heavy chain (KHC), a plus end-directed motor. This posterior localization is abolished in grk mutants that no longer maintain the microtubule (MT) gradient in the oocyte. To test the hypothesis that Nod binds to the plus ends of MTs, we expressed and purified both full-length Nod ($Nod_{FL}$) and a truncated form of Nod containing only the motorlike domain ($Nod_{318}$) from *Escherichia coli* and assessed their interactions with MTs in vitro. Both $Nod_{FL}$ and $Nod_{318}$ demonstrate preferential binding to the ends of the MTs, displaying a strong preference for binding to the plus ends. When $Nod_{318}$-GFP:MT collision complexes were trapped by glutaraldehyde fixation, the preference for binding to plus ends versus minus ends was 17:1. $Nod_{FL}$ and $Nod_{318}$ also promote MT polymerization in vitro in a time-dependent manner. The observation that Nod is preferentially localized to the plus ends of MTs and stimulates MT polymerization suggests a mechanism for its function.**

## INTRODUCTION

In *Drosophila melanogaster* female meiosis, the controlled movement of achiasmate chromosomes on the meiotic spindle is dependent on Nod, a 666 amino acid kinesinlike protein that localizes along the arms of meiotic chromosomes (Zhang *et al.,* 1990; Afshar *et al.,* 1995a, 1995b; see Figure 1B). In the absence of functional Nod protein, achiasmate chromosomes dissociate from the main chromosome mass immediately after nuclear envelope breakdown (NEB) by migrating off the ends of the developing spindle (Theurkauf and Hawley, 1992). Both genetic and cytological studies suggest that Nod functions to hold chromosomes at or near the metaphase plate, opposing the poleward force exerted by the kinetochores (Theurkauf and Hawley, 1992; Matthies *et al.,* 1999). Given that the microtubules (MTs) in the oocyte spindle are arranged with their plus ends at or near the metaphase plate (Riparbelli and Callaini, 2005), these results initially suggested that Nod acted as a plus end-directed motor that pushes chromosomes toward the metaphase plate (Matthies *et al.,* 1999). A function of Nod in pushing chromosomes arms toward the metaphase plate has also been demonstrated in *Drosophila* mitotic cells by Goshima and Vale (2003). These authors have shown that in cells in which Nod function is ablated by RNAi, the arms of most chromosomes were extended along the spindle axis toward one of the two poles rather than being held at or near the metaphase plate.

However, several lines of evidence show that the motorlike domain of Nod lacks the capacity for vectorial transport (Matthies *et al.,* 2001). First, Nod lacks three major structural elements that are found in virtually all kinesins (the neck, the neck-interactor region, and a crucial salt bridge) and are required for movement (Rice *et al.*, 1999; Case *et al.,* 2000). Second, although the motorlike domain of Nod is 34% identical to the prototypical human kinesin heavy chain protein (Hs KHC) motor domain, when one considers only residues that are strongly conserved within the KHC superfamily, 12 of the 62 fully conserved amino acids are changed in Nod, and 6 of the 51 strongly similar amino acids are different in Nod (Matthies *et al.,* 2001). Similarly, with respect to the 10 residues in Hs KHC that are most critical for MT binding (Woehlke *et al.,* 1997), 7 of these amino acids are altered in Nod. Third, although MTs activate the ATPase activity of Nod more than 2000-fold (Matthies *et al.,* 2001), this ATPase activity is not coupled to vectorial movement (i.e., Nod does not produce MT gliding in vitro; Matthies *et al.,* 2001). Fourth, the substitution of a single amino acid in the ATP-binding motif of *Drosophila* KHC with the analogous amino acid from Nod results in a drastic inhibition of motility

This article was published online ahead of print in *MBC in Press* (http://www.molbiolcell.org/cgi/doi/10.1091/mbc.E05–06–0582) on September 7, 2005.

[D] The online version of this article contains supplemental material at *MBC Online* (http://www.molbiolcell.org).

‡ These authors contributed equally to this work.

Address correspondence to: R. Scott Hawley (rsh@stowers-institute.org).

Abbreviations used: MT, microtubule; GFP, green fluorescent protein; KHC, kinesin heavy chain; NEB, nuclear envelope breakdown.

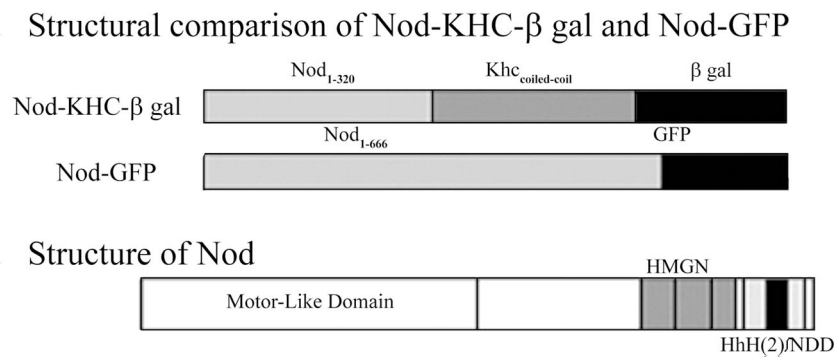


**Figure 1.** The structure of the *Drosophila* Nod kinesinlike protein. (A) A schematic comparison of the structure of the $Nod_{FL}$-GFP protein expressed for these studies and the Nod-KHC-$\beta$gal fusion protein studied by Clark *et al.* (1997). Light gray blocks denote Nod sequences, dark gray blocks denote the KHC component of the Nod-KHC-$\beta$gal fusion protein, and black regions denote the $\beta$gal or GFP tags. The motorlike domain of Nod falls entirely within the first 320 amino acids at the N-terminus. (B) A drawing of the Nod protein indicating the position of the motor domain, the three HMGN domains, and the HhH(2)/NDD domain. The HMGN and HhH(2)/NDD domains are involved in binding Nod to chromosomes (Afshar *et al.*, 1995b; Cui and Hawley, 2005).

(Matthies *et al.*, 2001). Thus, Nod's ability to hold chromosomes on the meiotic spindle is unlikely to result from any innate ability to move chromosomes along MT tracks. Although the ability of Nod to hold chromosomes in position might reflect its ability to bridge chromosome arms to the plus ends of nonkinetochore MTs in the spindle and hold them in place, MT tread-milling would presumably draw chromosomes to the poles of the meiotic spindle rather than pushing them toward the metaphase plate.

To better understand how Nod can generate poleward force, it would be helpful to understand how the Nod protein interacts with both chromosomes and MT filaments. In a companion article (Cui and Hawley, 2005), we show that the binding of Nod to the oocyte chromosomes requires the activity of a specific C-terminal motif, referred to as an HhH(2)/NDD domain, which may mediate either Nod:DNA or Nod:protein interactions. In this article we focus on determining the manner in which Nod interacts with the MTs. Unfortunately, previous studies of the ability of Nod, or parts of Nod, to localize on microtubule arrays of known polarity within cells have provided confusing results with respect to this question. Clark *et al.* (1997) demonstrated that a Nod-KHC-$\beta$gal fusion protein containing the Nod motorlike domain fused to the coiled coil domain of KHC and $\beta$-galactosidase (see Figure 1A) functions as an in vivo reporter for the minus ends of MT arrays. However, using a similar in vivo assay, we show below that full-length Nod-GFP protein, which retains full biological function, localizes in a manner similar to that exhibited by the plus end-directed motor KHC (Clark *et al.*, 1997, Brendza *et al.*, 2000).

To directly determine whether or not Nod binds to the ends of MTs, and if so, to which end, we have examined the interactions of purified full-length Nod ($Nod_{FL}$) and the Nod motorlike domain ($Nod_{318}$) with MTs in vitro. We demonstrate that both $Nod_{FL}$ and $Nod_{318}$ bind preferentially to the plus ends of the MT and promote MT polymerization. As discussed below, the observation that Nod localizes preferentially to the plus end of MTs suggests a mechanism for its function, similar to the clamped-filament elongation model proposed for actin-based motors (Dickinson and Purich, 2002). This mechanism provides a means for explaining the ability of a protein like Nod, which lacks the capacity for vectorial transport, to propel chromosomes toward the metaphase plate.

## MATERIALS AND METHODS

### *Construction of $Nod_{FL}$-GFP Constructs for Transformation into* Drosophila

Full-length wild-type *nod* cDNA was amplified by PCR and a *Sma*I site was added on the 5′ end of the PCR product. The resulting sequence was cloned into a pEGFP-N1 vector (Clontech, Palo Alto, CA) *Sma*I site by blunt-end ligation to form a $Nod_{FL}$-GFP fusion gene. Subsequently, the $Nod_{FL}$-GFP coding sequence was released by digestion with *Kpn*I and *Bam*HI and ligated into the pUASp vector (a generous gift from Dr. Pernille Rørth; Rørth, 1998) double-digested with *Kpn*I and *Bam*HI to form pUASp-$Nod_{FL}$-GFP. The entire coding sequence was verified on both strands.

### *Construction of Bacterial Expression Vector Encoding $Nod_{FL}$-GFP*

The $Nod_{FL}$-GFP coding sequence was amplified from pUASp-$Nod_{FL}$-GFP using the primers 5′-ACGCGTCGACGTGGCATGGAGGGCGCCAAATTAAGGCG -3′ and 5′-AAGGAAAAAAGCGGCCGCCTTGTACAGCTCGTCCATGCCG-3′. This PCR product was digested with *Sal*I and *Not*I and ligated into pET-21a (Novagen, Madison, WI), keeping the coding sequence in frame with the T7 and 6xHis tags. The T7 tag was subsequently removed by *Nhe*I and *Sal*I double digestion of the vector and replaced with the sequence encoding a Flag tag (DYKDDDDY) using the same sites to form pET-$Nod_{FL}$-GFP.

### *Construction of Bacterial Expression Vectors Encoding $Nod_{318}$ and $Nod_{318}$-GFP*

The sequence encoding the N-terminal 318 amino acids of Nod ($Nod_{318}$) was amplified from wild-type *nod* cDNA using the primers 5′-ACGCGTCGACGTGGCATGGAGGGCGCCAAATTAAGGCG -3′ and 5′-AAGGAAAAAAGCGGCCGCCTTGGCACTGGTGCCAAAACGC-3′ and double-digested with *Sal*I and *Not*I. The $Nod_{FL}$-GFP coding sequence in the pET-$Nod_{FL}$-GFP construct was removed by double digestion with *Sal*I and *Not*I and the digested $Nod_{318}$ PCR product was then cloned into the linearized vector using the *Sal*I and *Not*I sites.

To make a $Nod_{318}$-GFP bacterial expression vector, the sequence encoding $Nod_{318}$ was amplified from wild-type *nod* cDNA with the primers: 5′-ACGCGTCGACGTGGCATGGAGGGCGCCAAATTAAGGCG-3′ and 5′-CGCGGATCCCGCTTGGCACTGGTGCCAAAACGCAG-3′ and double-digested with *Sal*I and *Bam*HI. The pET-$Nod_{FL}$-GFP construct was double-digested with *Sal*I and *Bam*HI to remove the $Nod_{FL}$ cDNA sequence and the digested $Nod_{318}$ PCR product was cloned into the *Sal*I and *Bam*HI sites. For each of the expression constructs, the entire coding sequence was verified on both strands.

### *Expression and Purification of Bacterial Expressed Proteins*

pET21a vectors carrying constructs encoding either $Nod_{FL}$-GFP, $Nod_{318}$-GFP, or $Nod_{318}$ were transformed into BL21(DE3) competent cells (Invitrogen, Carlsbad, CA). A single colony was picked and grown in 2 ml of LB medium plus 100 $\mu$g/ml ampicillin at 37°C, shaken at 250 rpm overnight. One milliliter of bacteria culture was added to 100 ml of LB medium plus 100 $\mu$g/ml ampicillin and grown at 37°C overnight at 250 rpm. Ten milliliters of the 100-ml culture was added to 500 ml LB medium plus 100 $\mu$g/ml ampicillin and grown at 37°C to reach $OD_{600}$ of 0.6. Protein expression was induced by adding 1 mM isopropyl-beta-D-thiogalactopyranoside (IPTG). The bacterial cultures were continuously grown at 20°C for another 4 h. The bacteria were harvested at 6000 rpm for 30 min at 4°C, and the bacterial pellets were stored at −80°C.

The *E. coli* pellets were resuspended in ice-cold native binding buffer (20 mM Tris, pH 8.0, 500 mM NaCl, 10 mM imidazole, 20 mM $\beta$-mercaptoethanol, 1% Triton X-100, 10% glycerol, 10 mM ATP, 0.1 mM AEBSF, 1 $\mu$g/ml aprotinin, 1 $\mu$g/ml pepstatin, 1 $\mu$g/ml leupeptin) at 5 g/ml. Lysozyme at 1 mg/ml was added to the solution and incubated on ice for 30 min. The solution was passed through a precooled French press twice at 1200–1300 psi. The lysates were treated with DNAse I (5 $\mu$g/ml) and RNAse A (10 $\mu$g/ml) on ice for 15–20 min. The lysates were then centrifuged at 18,000 rpm for 30 min at 4°C.

Supernatants were saved and incubated with Ni-NTA agarose beads (Invitrogen) in a 50-ml conical tube with mixing for 2 h at 4°C. The Ni-NTA agarose beads were pelleted at 800 × *g* for 2 min at 4°C and washed in ice-cold washing buffer (20 mM Tris, pH 8.0, 1000 mM NaCl, 20 mM imidazole, 20 mM β-mercaptoethanol, 1% Triton X-100, 10% glycerol) four times in the 50-ml conical tube. In the last wash, the Ni-NTA agarose beads were loaded onto a 10-ml purification column and eluted with elution buffer (20 mM Tris, pH 8.0, 500 mM NaCl, 10% glycerol, and 200 mM imidazole). The eluates were dialyzed against ATPase buffer (20 mM HEPES, pH 7.3, 5 mM magnesium acetate, 0.1 mM EDTA, 0.1 mM EGTA, 1 mM dithiothreitol [DTT], 5% sucrose, 150 mM NaCl, and 50 mM potassium acetate), concentrated using Microcon Centrifugal Filter Devices (Millipore, Bedford, MA), and the protein concentration was measured using a Bradford protein assay (Bio-Rad Laboratories, Richmond, CA).

### *End Binding Assay*

To make polarity marked MTs, both rhodamine-labeled and unlabeled tubulin (Cytoskeleton, Denver, CO) were thawed, adjusted to 1 mM MgGTP, cold-depolymerized, and clarified by centrifugation for 15 min at 14,000 rpm at 4°C. MT seeds were assembled with equal volumes of 20 μM fluorescent rhodamine-labeled and unlabeled tubulin in the presence of 6 μM taxol (paclitaxel, Sigma-Aldrich, St. Louis, MO) at 34°C for 10 min. The highly fluorescent MT seeds were sheared with a 23-gauge needle (Becton Dickinson, Lincoln Park, NJ) and incubated with 20 μM fluorescent labeled and unlabeled tubulin at the ratio of 1:5 in the presence of 6 μM taxol at 34°C for 10 min. MTs were centrifuged at 14,000 rpm for 15 min at room temperature and resuspended in seed buffer (10 mM Pipes, pH 6.9, 5 mM $MgCl_2$, 1 mM EGTA, 6 μM taxol, 1 mM DTT, and 0.1 mM MgGTP).

$Nod_{FL}$-GFP or $Nod_{318}$-GFP proteins were allowed to bind to MTs in the presence of 1 mM MgAMPPNP (10 mM PIPES, pH 6.9, 5 mM $MgCl_2$, 1 mM EGTA, 6 μM taxol, 0.05 mM DTT, and 0.5 mM MgGTP), and the MT-Nod complexes were flowed into perfusion chambers (Cytoskeleton). After the MT-Nod complexes settled onto the coverslip, unattached MTs were removed by washing with 8 μl of oxygen-scavenging mix (OSM; 10 mM PIPES, pH 6.9, 5 mM $MgCl_2$, 1 mM EGTA, 1.5 mM MgAMPPNP, 1.5 mM magnesium acetate, 1 mg/ml bovine serum albumin, 0.2 mg/ml glucose oxidase, 33 μg/ml catalase, 25 mM glucose, 19.2 μg/ml phosphocreatine kinase, 4 mM phosphocreatine). The MT-Nod complexes were imaged by fluorescence microscopy, and the resulting data were deconvolved using the Softworx package (Applied Precision, Issaquah, WA). The two controls for this experiment are denoted as "no motor" and "GFP." The no motor control consists of assaying the MT polymerization mix with no added Nod protein. The GFP control consist of adding recombinant green fluorescent protein (rGFP), which was also expressed in *E. coli* and obtained from (BD Biosciences-Clontech, San Jose, CA).

Additional experiments were performed to determine whether there was a preference for Nod binding to the MT plus- or minus-end. Following the protocols of Sproul *et al.* (2005), the MTs were assembled as described above to obtain polarity marked MTs. The MT•Nod complex (500 nM tubulin, 3 μM taxol, 25 nM $Nod_{318}$-GFP) was preformed in a 10-μl aliquot and immediately fixed in 10 volumes of 1% glutaraldehyde in PME (3 μl of the original 10-μl reaction plus 30 μl of 1% glutaraldehyde). An additional 800 μl of PME buffer was added to yield a total volume of 833 μl. An aliquot of 50 μl of the 833-μl reaction was centrifuged through a 10% glycerol cushion onto round 1-mm poly-L-lysine coated glass coverslips. Nod binding was scored as motor binding to the MT end, the MT lattice, or both the MT end and MT lattice, and the binding events on polarity marked MTs were scored for plus- or minus-end binding.

### *Visual and Sedimentation Analysis of MT Polymerization*

For qualitative visual analysis of the polymerization of MTs, both rhodamine-labeled and unlabeled tubulin were thawed, adjusted to 1 mM MgGTP, cold depolymerized, and clarified by centrifugation for 15 min at 14,000 rpm at 4°C. The soluble tubulin was mixed to obtain a final ratio of 1:10 rhodamine-labeled:unlabeled tubulin and adjusted to 20 μM tubulin. Nod proteins at 0 or 50 nM protein were mixed with 3 μM of soluble tubulin in the presence of 1 mM MgATP (or MgAMPPNP), 1 mM MgGTP, and 1.5 μM taxol in PME80 (80 mM PIPES, pH 6.9, 5 mM $MgCl_2$, 1 mM EGTA). The final volume of the reaction was 150 μl. Reactions were initiated by the addition of soluble tubulin to the mix. At the predetermined time points, 8 μl was taken from the tube and perfused into the observation chamber. Five fields per time point (15-min intervals) were then imaged on an Olympus BX60 epifluorescence microscope (Melville, NY) using a 100× oil immersion objective. Digital images were captured with a Hamamatsu 4742 CCD camera (Bridgewater, NJ) in conjunction with QED In Vivo imaging software (Media Cybernetics, Silver Spring, MD).

For the sedimentation assays to assess MT polymerization, tubulin was treated as described above. Soluble tubulin at 3 μM was incubated with 1.5 μM taxol, 1.5 mM MgATP, 1.5 mM MgGTP in the presence or absence of $Nod_{FL}$-GFP or $Nod_{318}$ (0.15 μM of $Nod_{FL}$-GFP and 0.3 μM of $Nod_{318}$) at 34°C for 0–10 min, and then the solution was centrifuged in the Airfuge (Beckman Coulter, Fullerton, CA) at 20 psi for 30 min. The resulting supernatant and pellet for each reaction were analyzed by SDS-PAGE followed by Coomassie Brilliant Blue staining. The density of the protein bands was measured using Scion Image (Frederick, MD). To verify that the pellets represented MTs, we used rhodamine-labeled and unlabeled tubulin at the ratio of 1:15 and repeated the sedimentation assay. We resuspended the labeled MT pellets in PME80 buffer and evaluated the suspension by fluorescence microscopy.

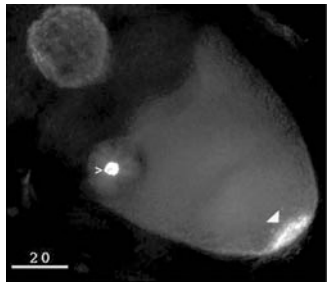


**Figure 2.** $Nod_{FL}$-GFP localizes to both the oocyte chromosomes and to the posterior pole in stage 9 oocytes. Otherwise wild-type oocytes expressing $Nod_{FL}$-GFP were stained with anti-GFP antibody and analyzed by deconvolution microscopy. The open arrowhead indicates $Nod_{FL}$-GFP localization to the oocyte chromosomes. The filled arrowhead indicates $Nod_{FL}$-GFP localization to the posterior pole of the oocyte. Scale bar, 20 μm.

### *Statistical Analysis of Polymerization Data*

For the sedimentation assays designed to assess MT polymerization, each experiment was run in duplicates, and three independent experiments were performed. The statistical differences between control samples and Nod-treated samples were calculated by Microsoft Excel (Redmond, WA) Student's *t*-test. Error bars in Figures 8 and 9 denote the SE of the mean.

### *Fly Stocks*

The pUASp-$Nod_{FL}$-GFP construct was introduced into *Drosophila* by P element-mediated transformation. Germline expression of $Nod_{FL}$-GFP was achieved by expressing the *P{UASp-Nod$_{FL}$-GFP}* construct under the control of the *nanos-Gal4::VP16* driver (Van Doren *et al.*, 1998). $grk^{DC}$ and $grk^{2EB}$ flies were kindly provided by Dr. Trudi Schüpbach (Princeton University).

### *Genetic Crosses*

We introduced *P{UASp-Nod$_{FL}$-GFP}* carrying chromosomes into the *grk* genetic background to examine $Nod_{FL}$-GFP localization. Cross 1: $w^{1118}$*; Sp/SM1; Pr Bsb/TM3* virgin females were crossed with *+/Y; grk/SM1* males. Crosses 2 and 3: $w^{1118}$*/Y; Sp/SM1; Pr Bsb/TM3* males were crossed with *y w/y w; P{UASp-Nod$_{FL}$-GFP}/P{UASp-Nod$_{FL}$-GFP}* and *y w/y w; P{nanos-Gal4::VP16}/P{nanos-Gal4::VP16}* virgin females, respectively. The offspring from Cross 1 were intercrossed to generate $w^{1118}$*; grk/SM1; Pr Bsb/TM3* flies. Similarly, the offspring from each of Crosses 2 and 3 were intercrossed to generate $w^{1118}$*/y w; Sp/SM1; P{UASp-nod-GFP}/P{UASp-nod-GFP}* and $w^{1118}$*/y w; Sp/SM1; P{nanos-Gal4::VP16}/P{nanos-Gal4::VP16}* flies. Subsequently, $w^{1118}$*/Y; grk/SM1; Pr Bsb/TM3* male flies were crossed with either $w^{1118}$*/y w; Sp/SM1; P{UASp-Nod$_{FL}$-GFP}/P{UASp-Nod$_{FL}$-GFP}* or $w^{1118}$*/y w; Sp/SM1; P{nanos-Gal4::VP16}/P{nanos-Gal4::VP16}* virgin females. Then the offspring from the above two crosses were mated each other to generate ($w^{1118}$*/w$^{1118}$ (or w$^{1118}$/y w); grk$^{DC}$/grk$^{2EB}$; P{UASp-Nod$_{FL}$-GFP}/P{nanos-Gal4::VP16}* female flies. Ovaries from these females and *grk/+* controls were dissected and stained with anti-GFP antibody as described in Cui and Hawley (2005).

## RESULTS

### *Functional $Nod_{FL}$-GFP Localizes to the Posterior Pole of Stage 9 Oocytes in a Manner That Requires a Properly Organized MT Network*

When expressed in *nod* mutant oocytes under the control of the germline-specific *nanos-Gal4::VP16* driver, the $Nod_{FL}$-GFP protein localizes to oocyte chromosomes and fully rescues the defective chromosome segregation phenotype exhibited by *nod* oocytes (Cui and Hawley, 2005). We show here that $Nod_{FL}$-GFP also accumulates at the posterior pole of stage 9 oocytes, as shown in Figure 2. This pattern parallels the localization pattern observed for KHC, a known plus

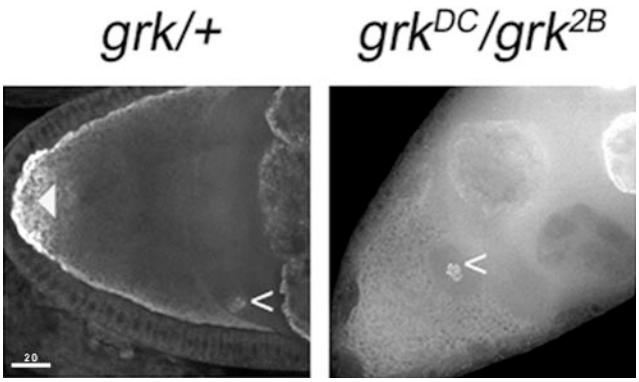


**Figure 3.** Localization of $Nod_{FL}$-GFP in stage 9 oocytes in which the MT organization is disrupted by mutations in *grk*. Normal (*grk*/+) and *grk* ($grk^{DC}/grk^{2B}$) oocytes expressing $Nod_{FL}$-GFP were stained with anti-GFP antibody (GFP) and analyzed by deconvolution microscopy. The open arrowhead indicates $Nod_{FL}$-GFP localization to the oocyte chromosomes. The filled arrowhead indicates $Nod_{FL}$-GFP localization to the posterior pole of the oocyte. Note that $Nod_{FL}$-GFP localizes to the oocyte chromosomes in both *grk*/+ and *grk* oocytes, but only localizes to the posterior pole in *grk*/+ oocytes. Scale bar, 20 $\mu$m.

end-directed motor (Clark *et al.*, 1997; Brendza *et al.*, 2000), but contrasts with that of a Nod-KHC-$\beta$gal fusion protein, which localizes to the minus ends of MT arrays (Clark *et al.*, 1997). The contradiction between our observations and the localization of Nod-KHC-$\beta$gal may be resolved by supposing that some component of the Nod-KHC-$\beta$gal fusion protein other than the Nod motorlike domain, perhaps the KHC sequences, is responsible for minus end-directed localization.

To determine whether the localization of Nod to the posterior pole of stage 9 oocytes requires the integrity of the oocyte MT network, we localized $Nod_{FL}$-GFP in $grk^{2B}/grk^{DC}$ mutant oocytes. Jauschke *et al.* (2002) demonstrated that the normal organization of MTs in stage 9 oocytes is abolished in $grk^{2B}/grk^{DC}$ mutants, as visualized using the MT-associated protein Tau-GFP. Although cytoplasmic $Nod_{FL}$-GFP is localized at the posterior pole in *grk* heterozygous stage 9–10A oocytes, this localization was abolished in $grk^{2B}/grk^{DC}$ mutant oocytes. Instead, $Nod_{FL}$-GFP was dispersed throughout the entire egg chamber (Figure 3). These results suggest that $Nod_{FL}$-GFP accumulation at the posterior pole is dependent on proper MT organization within the oocyte.

However, several lines of evidence suggest that interpreting the significance of this localization in terms of the manner in which Nod interacts with microtubules must be done with some caution. First, the minus-end motor dynein also concentrates at the posterior (Li *et al.*, 1994), albeit in a manner that depends on the function of KHC (Brendza *et al.*, 2002). Second, microtubule imaging shows no evidence of microtubules plus ends being concentrated at the posterior pole. Indeed, although minus ends are highly concentrated at the anterior of the oocyte and near the cortex, the posterior pole is relatively free of microtubules (Cha *et al.*, 2002). Both Cha *et al.* (2002) and Serbus *et al.* (2005) have proposed elegant models to explain these discrepancies while still proposing that KHC localizes to the posterior pole because of its capacity to act as a plus end-directed motor and thus push away from the minus ends concentrated at the anterior pole and along the cortex. However, these observations at least raise the possibility that the processes that localize Nod to the posterior pole may not be completely dependent on direct interactions of Nod with the MT. Indeed, Cui and Hawley (2005) have shown that localization of full-length Nod to the posterior pole of the oocyte also requires a functional HhH(2)/NDD DNA-binding domain, raising the possibility that this domain mediates the interaction of Nod with at least one other protein. Thus, in order to directly assess the ability of Nod to bind to the plus ends of MTs we pursued a more direct in vitro approach for studying Nod-MT interactions.

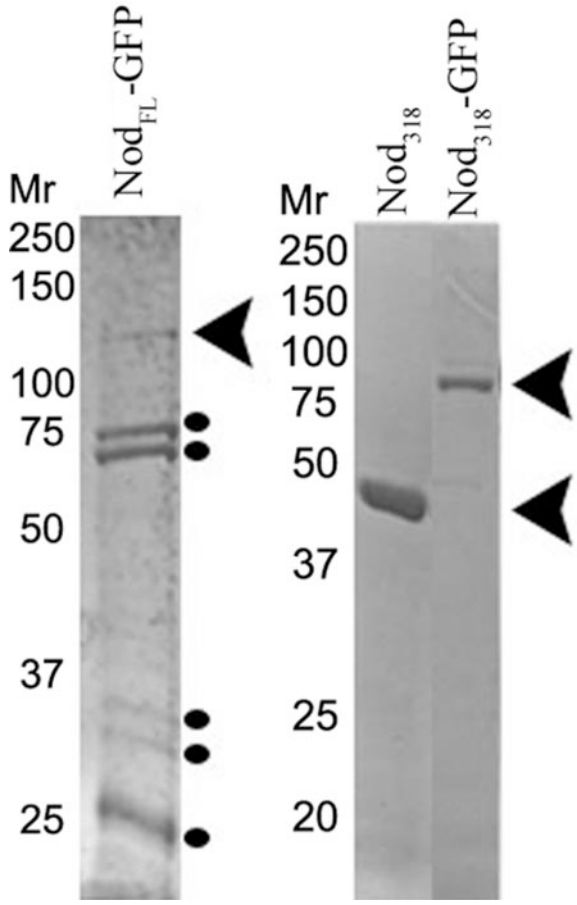


**Figure 4.** Purification of $Nod_{FL}$-GFP, $Nod_{318}$, and $Nod_{318}$-GFP from *E. coli*. Full-length ($Nod_{FL}$) or motor domain ($Nod_{318}$) constructs were expressed in *E. coli* and purified using Ni-NTA agarose beads. Shown are Coomassie blue-stained SDS-PAGE gels of purified proteins. The (▶) denote the full-length proteins, whereas the (●) indicate breakdown products or contaminants. Based on Western blot analysis (unpublished data), the majority of the lower molecular weight bands appear to be the result of breakdown or proteolysis of the Nod-GFP proteins.

### *$Nod_{FL}$ and $Nod_{318}$ Show Preferential Binding to MT Plus Ends In Vitro*

The MT-dependent localization of $Nod_{FL}$-GFP to the posterior pole suggested that Nod might either be moved to or preferentially binds the plus ends of MTs. To test this possibility, we purified bacterially expressed $Nod_{FL}$-GFP and $Nod_{318}$-GFP proteins, incubated them with polarity marked MTs, and visually assessed the position of Nod binding along the length of the MT. Figure 4 shows the expressed and purified proteins used for these in vitro assays. Although we were successful in purifying $Nod_{318}$ and $Nod_{318}$-GFP to >99% homogeneity, the purification of the full-

length Nod construct ($Nod_{FL}$-GFP) was more problematic. As shown in Figure 4, several additional proteins copurified with $Nod_{FL}$-GFP. Based on Western blot analysis (unpublished data), the majority of the lower molecular weight bands appear to be the result of breakdown or proteolysis of the $Nod_{FL}$-GFP protein.

To determine the ability of these proteins to bind to MTs, we coincubated $Nod_{FL}$-GFP and $Nod_{318}$-GFP with rhodamine-labeled MTs. A substantial fraction of these MTs were polarity-marked such that the brighter region of fluorescence corresponds to the minus end of the MT while the fainter region corresponds to the region including the plus end (see Figure 5A). We then visualized Nod binding to MTs by measuring the number and position of GFP foci (corresponding to sites of $Nod_{FL}$-GFP and $Nod_{318}$-GFP binding) along the length of the MTs by fluorescence microscopy. As expected, no foci were observed in the "no motor" control. Furthermore, binding of GFP protein lacking Nod sequences to MTs in this assay was rare, even at high concentrations of protein (57.2 nM), and no instances of end-binding to single MTs were observed. The one example of GFP binding observed involved a GFP focus localized to a site at which the lattices of three MTs appeared to intersect. However, for both $Nod_{FL}$-GFP and $Nod_{318}$-GFP, Nod-MT complexes were observed and their frequency increased with the concentration of the Nod-GFP protein. $Nod_{318}$-GFP binds to 2.3–6.5% of MTs at concentrations of $Nod_{318}$-GFP ranging from 6.1 to 24 nM, whereas $Nod_{FL}$-GFP binds to 3.3–24.4% of MTs at concentrations ranging from 0.19 to 18.9 nM. These observations demonstrate that the Nod-GFP proteins produced in *E. coli* retain their ability to bind MTs. Moreover, the observation that that $Nod_{FL}$-GFP protein binds to more MTs at lower concentrations of protein than does $Nod_{318}$-GFP suggests that the full-length $Nod_{FL}$-GFP protein has a higher affinity for MTs than does the $Nod_{318}$ protein, which carries only the motorlike domain of Nod.

We categorized the binding of Nod-GFP proteins to MTs into three classes: *end-binding* (see Figure 5, A–C), in which the GFP focus defined the end of the MT, *lattice binding* (see Figure 5, D–F), in which the GFP focus was positioned somewhere along the length of the MT, and *junctions* (Figure 5, G–I) in which the GFP focus marks a site of intersection between two MTs. In those cases in which the MT was polarity marked, end binding events could be further classified as plus or minus end bindings (see below). Although the images in Figure 5 portray MT-binding events for the $Nod_{FL}$-GFP protein, MT binding data for both $Nod_{FL}$-GFP and $Nod_{318}$-GFP are summarized in the table embedded in Figure 5. In the case of $Nod_{318}$-GFP, the majority of MT-binding events involved single MTs at all three concentrations tested, whereas for $Nod_{FL}$-GFP junction events involving two MTs were the most frequently observed class of Nod-MT interaction at all concentrations tested. We will first discuss the cases in which $Nod_{FL}$-GFP or $Nod_{318}$-GFP interacts with a single MT and then discuss interactions with MT junctions.

Figure 6 displays the MT binding events for both $Nod_{FL}$-GFP and $Nod_{318}$-GFP as a histogram of Nod-GFP localization along the MTs. The average length of these MTs is 5 $\mu$m. We separated the position of the Nod-GFP focus along the microtubule into seven "bins" to denote their position. The first bin, labeled "Tip", denotes those cases in which the Nod-GFP focus was located at a point between 0 and 7% of the of the length of the MT, and the second bin denotes those cases where the focus fell between 8 and 14% of the length of the MT, and so on. The last bin, labeled "Center," includes those GFP foci mapping close to or at the center of the MT. Because we are always measuring the distance from the GFP focus to the nearest end, the position of the focus cannot exceed 50% of the length of the MT. The bin size of seven reflects the fact that for foci denoted as lattice binding events which were close to, but not at, the tip, the distance from focus to tip was at least 7% of MT length. Foci <7% of MT length from the tips were considered end-binding events. Using this binning method to quantitate the position of the GFP focus on the MT, we found that both $Nod_{FL}$-GFP and $Nod_{318}$ -GFP show higher binding affinity to the end of the MT compared with any other location along the MT (see Figure 6). Evidence that the binding of Nod to the MT end occurs preferentially at the plus end is provided in the following section.

In addition to binding at the ends or along the lattice of MTs, $Nod_{FL}$-GFP and $Nod_{318}$-GFP were often observed to connect two MTs and form structures we denote as junctions (see Figure 5, G–I). The analysis of these junctions further supports our conclusion that Nod binds preferentially to MT ends and suggests that the C-terminal half of Nod also carries an MT-binding domain. The conclusion that the Nod binding in junctions is also often mediated by the binding to MT ends is based on an analysis of the structure of the junctions themselves. Junctions were observed either between two MT ends (with Nod at the junction), between an end and a lattice (as shown in Figure 5, G–I) or between two lattices. The 10 junctions with $Nod_{318}$-GFP foci may be further classified as 3 end-end junctions, 4 end-lattice junctions, and 3 lattice-lattice junctions. Thus, among the 20 MTs composing these 10 junctions, $Nod_{318}$-GFP is bound at the end of the MT in 50% of the cases. For $Nod_{FL}$-GFP, a total of 52 MTs were observed as components of 26 junctions. These 26 junction structures may be further classified as 8 end-end junctions, 13 end-lattice junctions, and 5 lattice-lattice junctions, such that of the 52 MTs involved, $Nod_{FL}$-GFP was bound to the end of the MT in 54.7% of the cases.

The argument that Nod possesses a second MT-binding domain within its C-terminus is based on the observation that $Nod_{FL}$-GFP protein clearly possesses a greater ability to bind to or create MT junctions (36–57%) than does the $Nod_{318}$-GFP protein (8–18%). This greater ability of $Nod_{FL}$-GFP to form or bind to junctions suggests that a second MT-binding domain might exist in the C-terminal half of Nod, such that the $Nod_{FL}$-GFP protein can bind more than one MT fiber. Such a secondary MT binding domain has been identified in the C-terminal (nonmotor) half of the HsKid protein, a human chromokinesin that is similar in structure to Nod (Shiroguchi *et al.*, 2003). Although the ability of Nod to form junctions might also be explained by an ability to form dimers, chromokinesins like Nod and HsKid lack the coiled coil domain that is believed to essential for dimerization (Shiroguchi *et al.*, 2003).

These data allow two general conclusions. First, both $Nod_{FL}$-GFP and $Nod_{318}$-GFP bind to MTs in vitro, with a strong preference for the ends of the MT. Second, $Nod_{FL}$-GFP has a higher affinity for MT-binding than does $Nod_{318}$-GFP, apparently as a consequence of a greater ability of $Nod_{FL}$-GFP to interconnect two MTs, a property that may reflect a secondary MT binding site in the C-terminus of Nod. However, even these junction events are also a manifestation of Nod's preferential ability to bind MT ends, because the majority of junctions involve at least one MT end.

### *Nod Binds Preferentially to the Plus Ends of MTs*

Using those cases in which $Nod_{FL}$-GFP or $Nod_{318}$-GFP localized to the end of a polarity marked MT, we were able to demonstrate that Nod preferentially binds to the plus ends

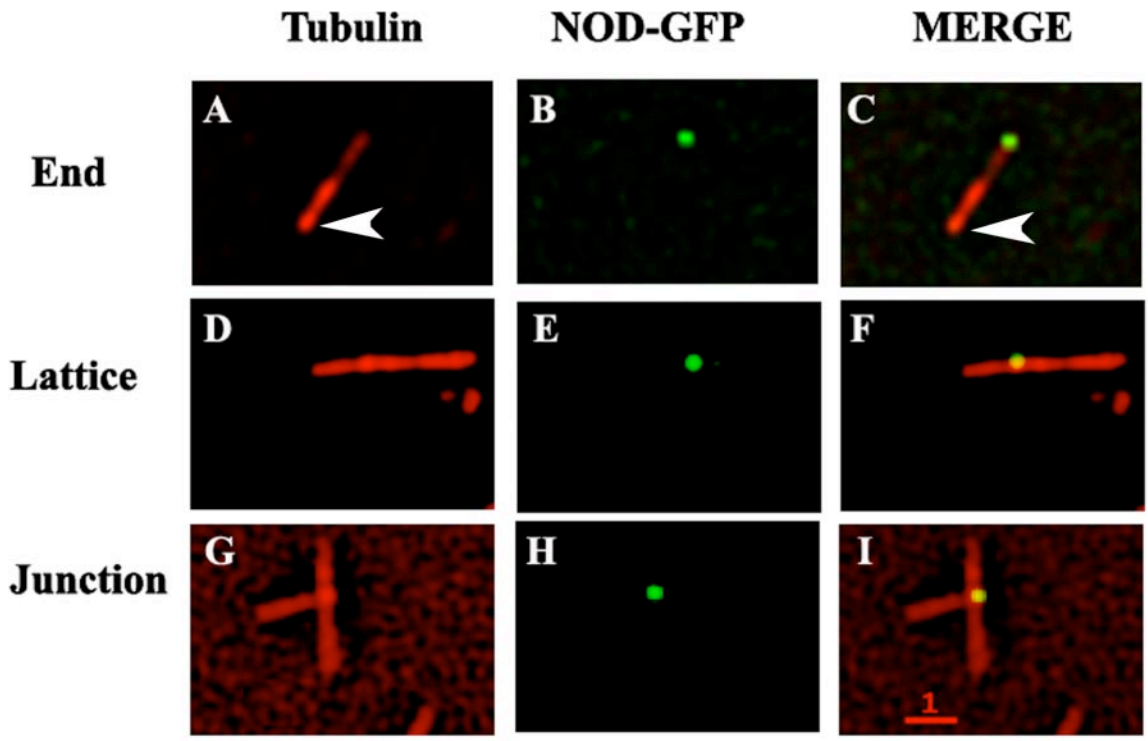


**Summary of Nod-microtubule binding**

| Nod | [Protein] nM | Total MT | % MT bound (#) | % Binding (#) Lattice | Junction | End |
|---|---|---|---|---|---|---|
| No motor | 0.0 | 335 | 0.0 (0) | 0.0 (0) | 0.0 (0) | 0.0 (0) |
| GFP | 28.6 | 535 | 0.0 (0) | 0.0 (0) | 0.0 (0) | 0.0 (0) |
| GFP | 35.8 | 423 | 0.2 (1) | 100.0 (1) | 0.0 (0) | 0.0 (0) |
| GFP | 57.2 | 763 | 0.4 (3) | 0.0 (0) | 100.0 (3) | 0.0 (0) |
| $NOD_{318}$-GFP | 6.1 | 1997 | 2.3 (45) | 42.2 (19) | 17.7 (8) | 40.0 (18) |
| $NOD_{318}$-GFP | 12.1 | 664 | 3.6 (24) | 33.3 (8) | 8.3 (2) | 58.3 (14) |
| $NOD_{318}$-GFP | 24.2 | 1179 | 6.5 (77) | 54.5 (42) | 10.3 (10) | 32.4 (25) |
| $NOD_{FL}$-GFP | 0.2 | 213 | 3.3 (7) | 14.2 (1) | 57.1 (4) | 28.4 (2) |
| $NOD_{FL}$-GFP | 1.0 | 427 | 6.3 (27) | 22.2 (6) | 44.4 (12) | 33.3 (9) |
| $NOD_{FL}$-GFP | 5.7 | 284 | 16.5 (47) | 25.5 (12) | 51.1 (24) | 23.4 (11) |
| $NOD_{FL}$-GFP | 18.9 | 135 | 24.4 (33) | 27.2 (9) | 36.4 (12) | 36.4 (12) |

* There are end-end, end-lattice and lattice-lattice junctions. All the MTs are counted in the junctions.

**Figure 5.** $Nod_{FL}$-GFP and $Nod_{318}$-GFP bind to MTs in vitro. (A, D, and G) Rhodamine-labeled MTs (red). (B, E, and H) $Nod_{FL}$-GFP localization (green). (C, F and I) Merge of the two channels showing $Nod_{FL}$-GFP localization on the MTs. (C) $Nod_{FL}$-GFP localizes to the plus end of a polarity-marked MT. The arrowhead denotes the minus end of the MT. (F) $Nod_{FL}$-GFP localizes to the lattice of a MT. (I) $Nod_{FL}$-GFP localized to the junction between MTs. The table summarizes MT binding scored for $Nod_{FL}$-GFP and $Nod_{318}$-GFP. Concentrations for $Nod_{FL}$-GFP and $Nod_{318}$-GFP are listed in the table; the tubulin concentration was 0.5 $\mu$M. As can be seen in D–F and G–I, GFP foci were often observed at "bright spots" of rhodamine-tubulin signal along the lengths or at the tips of MTs. Although these associations might indicate a higher concentration of tubulin oligomers at or near the site of Nod binding and the preference for Nod to bind at those sites, we note that "bright spots" are also commonly observed on MTs that do not have bound Nod protein, and thus they are not likely to be a consequence of Nod binding.

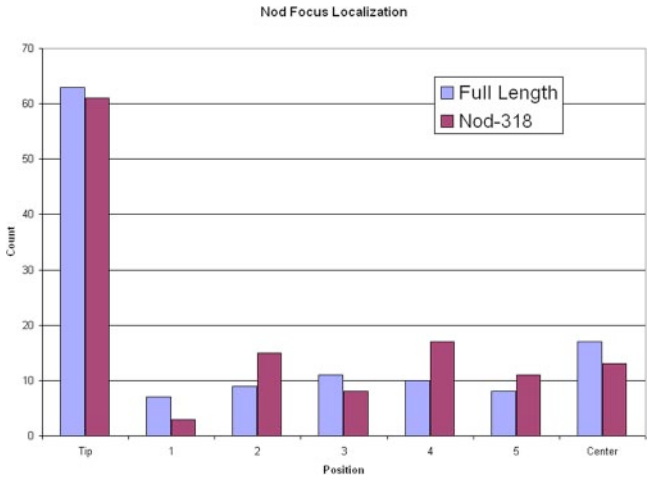


**Figure 6.** Distribution of Nod binding sites along MTs. The MT was divided into 7 segments from either end, such that 0 indicates either MT tip and 50, the center of the MT. Thus the first "bin" denotes those cases where the Nod focus fell at a point between 0 and 7% of the length of the microtubule, the second bin denotes those cases where the focus fell between 8 and 14% of the length of the microtubule, and so on. Because we are always measuring the distance from the GFP focus to the nearest tip of the MT the distance cannot exceed 50%. The bin size of seven reflects the fact that for those foci which were close to, but not at, the tip, the minimum distance from focus to tip was 7% of the length. The frequency of $Nod_{FL}$-GFP and $Nod_{318}$-GFP localization to each segment is plotted. The MTs scored for this localization are listed in the table in Figure 5.

of MTs. As shown in Figure 5, we found that Nod bound twice as frequently to the plus versus the minus end of the MT for both $Nod_{FL}$-GFP and $Nod_{318}$-GFP. The ratio of plus end/minus end binding events for $Nod_{FL}$-GFP was 15/8, and for $Nod_{318}$-GFP the ratio was 8/4. However, because the number of instances in which Nod was bound to the end of a polarity-marked MT was small, we repeated these experiments using a different method (glutaraldehyde fixation) for trapping the collision complex between $Nod_{318}$-GFP and polarity marked MTs. The results of this experiment are presented in Figure 7. In this experiment the frequency with which $Nod_{318}$-GFP bound to the MT end (71.8%) was approximately twofold higher than observed in the experiment presented in Figure 5, in which $Nod_{318}$-GFP was mixed with MTs only in the presence of AMPPNP. Moreover the ratio of plus-end (52) to minus end (3) binding events was ~17:1. The difference in these two sets of results likely reflects the fact that by mixing $Nod_{318}$-GFP and MTs in the presence of AMPPNP we are failing to trap the Nod complex at the site of the initial binding, and AMPPNP may be allowing Nod to migrate along the length of the MT. However, by fixing with glutaraldehyde immediately after mixing, as we do in Figure 7, we are capturing the initial sites of Nod MT interactions. Taken together, both experiments argue strongly that when binding to the MT end, Nod has a strong preference for the plus end.

### *$Nod_{FL}$-GFP and $Nod_{318}$ Promote MT Polymerization In Vitro*

The preferential binding of Nod to ends, and specifically the plus ends, of MTs suggested that Nod might play a role in controlling MT polymerization. To address this possibility, we set out to test the ability of $Nod_{FL}$-GFP and $Nod_{318}$ to facilitate this process. To test the ability of the Nod motorlike domain to mediate MT polymerization, we incubated $Nod_{318}$ with soluble rhodamine-labeled tubulin in the presence of MgATP or MgAMPPNP. At times 0 and 30 min, we visualized the presence or absence of polymerization by microscopic examination. As shown in Figure 8, there are many more MTs formed by 30 min in Nod-treated samples than are formed in the no motor control. The observation that Nod-promoted MT assembly occurred in the presence of either MgATP or MgAMPPNP suggests that $Nod_{318}$ does not require ATP turnover to promote MT polymerization. To control for the possibility that some of the observed MT polymerization might be due to the presence of bacterial proteins, we repeated this experiment by performing the MT polymerization experiment using extracts from *E. coli* cultures that did or did not express $Nod_{318}$. Although a high degree of MT polymerization was observed in the presence of $Nod_{318}$, little or no polymerization was observed in the presence of *E. coli* extract alone (see Supplementary Figure 1).

We used sedimentation analysis to quantify the ability of the Nod motorlike domain ($Nod_{318}$) and full-length Nod

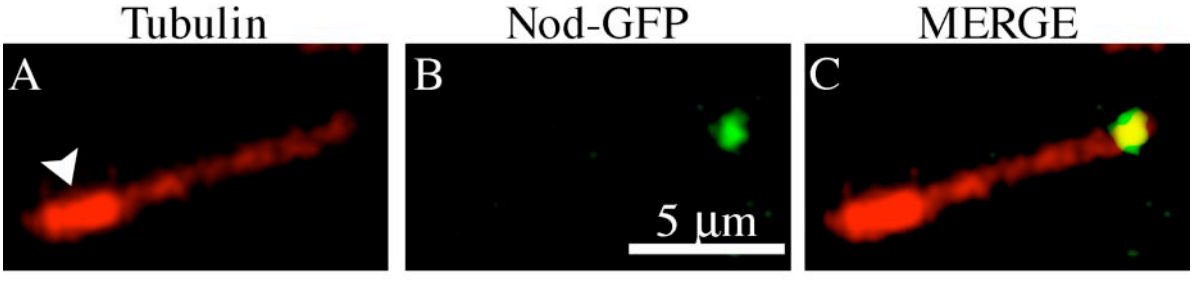


**Summary of Nod Binding Polarity Marked MTs**

| | Total MT | % MT Bound (#) | Lattice Binding (#) | Total End Binding (#) | Polarity Marked MTs % End Binding (#) | |
|---|---|---|---|---|---|---|
| | | | | | Plus End | Minus End |
| **25 nM $Nod_{318}$-GFP** | 6934 | 4.1 (234) | 28.2 (66) | 71.8 (168) | **31 (52)** | 1.8 (3) |

**Figure 7.** Trapping of the $Nod_{318}$-GFP collision complex by glutaraldehyde fixation. (A–C) A polarity marked MT denoted by a bright seed at the minus end (arrowhead in A) bound at the dimmer plus-end by $Nod_{318}$-GFP. The average length of the MTs counted was 4.63 ± 0.18 (SE). The tubulin concentration was 0.5 $\mu$M.

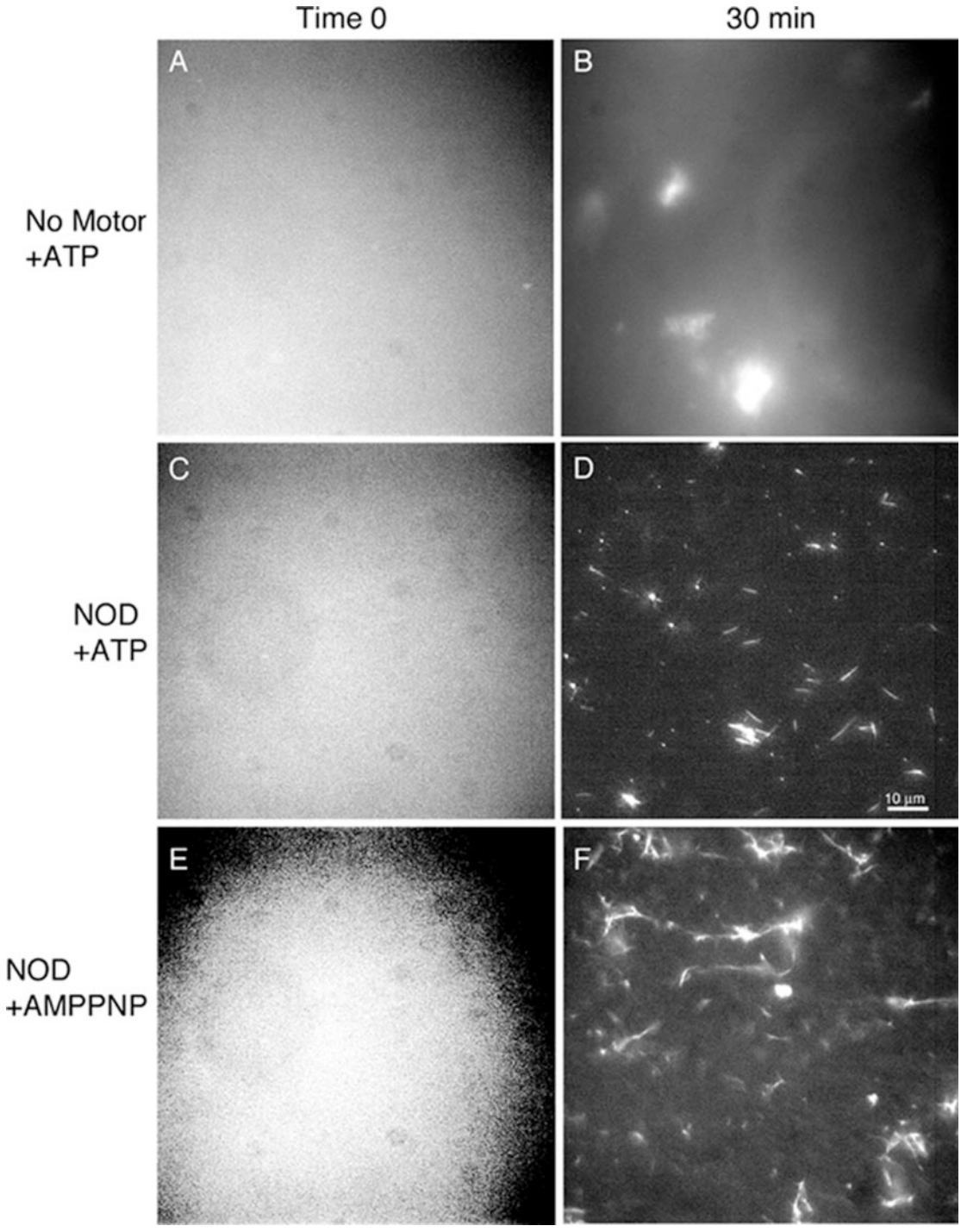


**Figure 8.** Nod promotes MT polymerization in vitro. Soluble labeled tubulin, 3 $\mu$M, was complexed with 50 nM $Nod_{318}$ in the presence of MgATP and the reaction was incubated for varying time points, at which time, 8 $\mu$l was extracted and MT polymerization was visually assayed on a fluorescence microscope. (A, C, and E) time 0; (B, D, and F) 30 min. (B) Little MT polymerization is observed in the absence of any motor; (D) In the presence of $Nod_{318}$ and MgATP, polymerization of individual MTs can be observed; (F) In the presence of $Nod_{318}$ and MgAMPPNP, polymerization is also seen with bundling of the MTs.

($Nod_{FL}$-GFP) to mediate MT polymerization. Soluble tubulin was incubated with or without $Nod_{FL}$-GFP or $Nod_{318}$, centrifuged, and subjected to SDS-PAGE to determine the fraction of tubulin that remained in the supernatant in comparison to the fraction that sedimented in the pellet. As shown in Figure 9A, both $Nod_{FL}$-GFP and $Nod_{318}$ result in a statistically significant increase ($p < 0.01$) in tubulin partitioning to the pellet when compared with the no motor controls. Similar results were also obtained using a $Nod_{318}$-GFP construct (unpublished data). To confirm that the partitioning of tubulin to the pellets represents Nod-promoted MT polymerization, we repeated the sedimentation assay

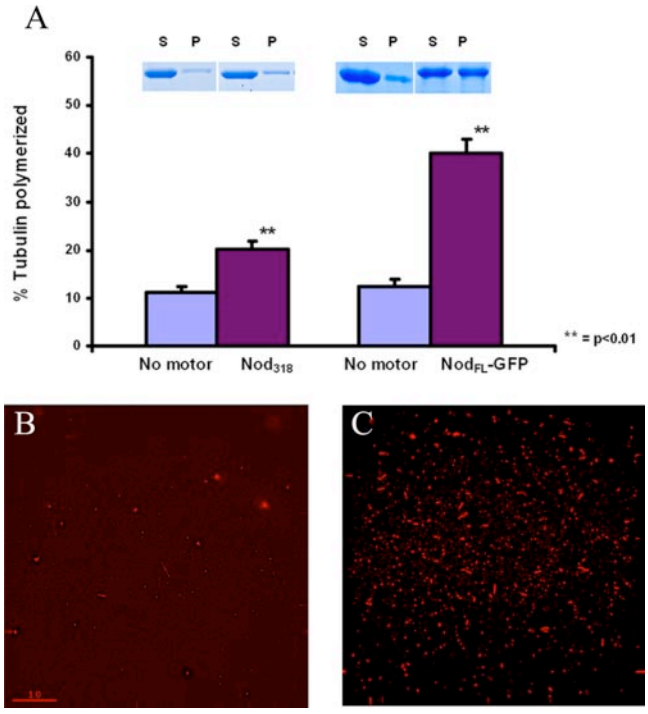


**Figure 9.** Sedimentation analysis of the effect of Nod on MT polymerization. (A) Both $Nod_{318}$ (300 nM) and $Nod_{FL}$ (150 nM) incubated with 3 $\mu$M soluble tubulin promote MT polymerization over time in the presence of MgATP. The reactions were centrifuged, and the supernatant and pellet at equal volume for each reaction were analyzed by SDS-PAGE. The amount of tubulin that partitioned to the supernatant and to the pellet were quantified (see gel slices). Error bars, SE of the mean. (B and C) To ensure that the tubulin that partitioned to the pellet was polymerized tubulin (MTs) and not aggregates of soluble tubulin, the experiment was repeated using rhodamine-tubulin, and the pellets were resuspended and examined using fluorescence microscopy. Each experiment was performed in duplicate on three separate occasions. The value presented in the histogram (A) is the average of those six repetitions. Error bars, SEM. The statistical differences between control samples and Nod-treated samples were calculated by Microsoft Excel Student's *t*-test.

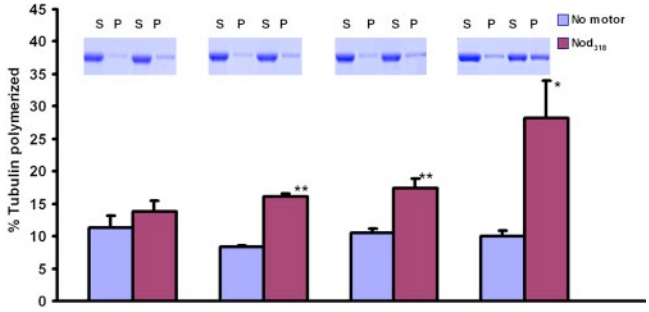


**Figure 10.** Nod promotes MT polymerization in a time-dependent manner. Soluble tubulin, 3 $\mu$M, and 300 nM $Nod_{318}$ incubated with MgATP polymerizes tubulin as a function of time as indicated by the increase of tubulin partitioning to the pellet (see gel slices). Each experiment was performed in duplicate on three separate occasions. The value presented in the histogram is the average of those six repetitions. Error bars, SEM. The statistical differences between control samples and Nod-treated samples were calculated by Microsoft Excel Student's *t*-test.

with fluorescently labeled tubulin and resuspended the pellets for direct microscopic examination. As shown for $Nod_{FL}$-GFP in Figure 9C, the resuspended pellets are comprised of large numbers of MTs rather than aggregates of soluble tubulin.

If Nod-promoted MT assembly is functionally significant, we would expect there to be a time-dependence to the process. Figure 10 shows $Nod_{318}$-promoted MT assembly using the sedimentation assay. The results reveal a significant increase ($p < 0.05$) in the fraction of tubulin that partitions to the pellet over time, whereas no increase in the fraction of tubulin sedimentation was seen in the absence of Nod. Therefore, Nod exerts its ability to stimulate MT polymerization in a time-dependent manner.

## DISCUSSION

The data presented above reveal two critical insights into Nod function: namely that full-length Nod localizes to the ends of MTs in vitro and that Nod promotes MT polymerization. Our conclusion that Nod binds preferentially to plus ends in vivo is supported by three observations: 1) Nod localizes to the posterior pole of stage 9 oocytes, in a manner similar to the plus-end-directed motor KHC; 2) the preferential binding of Nod to MT plus ends in vitro; and 3) Nod-promoted MT polymerization in vitro. Given that the MTs in the oocyte spindle are arranged with their plus ends at or near the metaphase plate (Riparbelli and Callaini, 2005), these data suggest a straightforward mechanism by which Nod, when bound to the arms of chromosomes, can generate the force required to push chromosomes arms toward the metaphase plate (Matthies *et al.*, 1999; Goshima and Vale, 2003). Indeed, we propose that Nod proteins bound along the arms of the chromosome cause the extension of MT plus ends by polymerization and that it is the growth in the MTs that serves to literally "push" those arms toward the metaphase plates. If correct, this mechanism provides at least one biochemical explanation for the "polar ejection force" (Rieder *et al.*, 1986).

In the experiments presented, Nod promotes polymerization of MTs in the presence of both MgATP and MgAMP-PNP, suggesting that ATP turnover is not required for the addition of tubulin subunits. This observation is perhaps not surprising given the observation by Matthies *et al.* (2001) that the affinity of Nod-ATP for MTs is similar to, and indeed slightly less than, the affinity of Nod-ADP for MTs. (Compare this to conventional kinesins in which the affinity of the motor-ATP complex for MTs is ~40–50 times greater than the affinity of the motor-ADP complex for MTs.) Nod ATPase activity may not be critical for the MT polymerization activity but it is essential for the ability of Nod to faithfully segregate chromosomes (Rasooly *et al.*, 1991, 1994; Matthies *et al.*, 2001). This apparent contradiction can be reconciled by the following model.

1) Nod MT polymerization activity also functions to stabilize the plus ends of growing MTs. Indeed, plus end binding proteins have this property (Howard and Hyman, 2003). In vivo, MTs are highly dynamic structures undergoing fluctuations between growth and rapid shortening; these dynamics are highly regulated by MT-binding proteins, which bind to the MT ends to facilitate stabilization or destabilization of the MT (Desai and Mitchison, 1997; Desai *et al.*, 1999, Howard and Hyman, 2003). Nod may act as a stabilizing protein by binding to the chromosomes with its C-terminus and to the MT plus end with its N-terminal kinesin motor domain.

2) By stabilizing the plus ends, Nod allows new tubulin dimers to be added to these ends. The addition of a new dimer leads to GTP hydrolysis in the MT polymer and a new GTP cap. This GTP cap may then be the new binding site for Nod.

3) ATP turnover by Nod could regulate in part the dynamics at the MT plus end by allowing Nod to detach from the elongated MT at the appropriate time and allowing rebinding to the plus end. This mechanism of binding the MT plus end, stabilizing the plus ends, then allowing subunit addition, would account for the in vivo observations that suggest Nod acts to "push" chromosomes away from the poles during meiotic spindle formation.

The various aspects of this model help to explain how Nod, a chromokinesin-like protein that lacks the capacity for vectorial transport, can nonetheless provide the force that maintains achiasmate chromosomes near the metaphase plate during spindle elongation at prometaphase I of meiosis.

## ACKNOWLEDGMENTS

We thank Dr. Tony Hyman for suggesting these experiments to us in the first place. We also thank Drs. Chieri Sato, Yong Cai, Jinji Jin, Joan Conaway, and Ron Conaway for their technical advice and consultation and Drs. Cathy Lake, Sue Jaspersen, Peter Baumann, Bill Gilliland, Scott Page, Wei Gong, and Youbin Xiang for helpful comments on the manuscript. The research was supported by the funds from the Stowers Institute for Medical Research, by a grant to R.S.H. from the National Science Foundation, and by a grant to S.P.G. from National Institute of General Medical Sciences, National Institutes of Health (GM54141).

## REFERENCES

Afshar, K., Barton, N., Hawley, R. S., and Goldstein, L.S.B. (1995a). DNA binding and meiotic chromosome localization of the *Drosophila* NOD kinesin-like protein. Cell *81*, 129–138.

Afshar, K., Scholey, J., and Hawley, R. S. (1995b). Identification of the chromosome localization domain of the *Drosophila* Nod kinesin-like protein. J. Cell Biol. *131*, 833–843.

Brendza, R. P., Serbus, L. R., Duffy, J. B., and Saxton, W. M. (2000). A function for kinesin I in the posterior transport of *oskar* mRNA and Staufen protein. Science *289*(5487), 2120–2122.

Brendza, R. P., Serbus, L. R., Saxton, W. M., and Duffy, J. B. (2002). Posterior localization of dynein and dorsal-ventral axis formation depend on kinesin in *Drosophila* oocytes. Curr. Biol. *12*(17),1541–1545.

Case, R. B., Rice, S., Hart, C. L., Ly, B., and Vale, R. D. (2000). Role of the kinesin neck linker and catalytic core in microtubule-based motility. Curr. Biol. *10*(3),157–160.

Cha, B. J., Serbus, L. R., Kappetsch, B. S., and Therkauf, W. E. (2002). Kinesin I-dependent cortical exclusion restricts pole plasm to the oocyte posterior. Nat. Cell Biol. *4*, 592–598.

Clark, I. E., Jan, L. Y., and Jan, Y. N. (1997). Reciprocal localization of Nod and kinesin fusion proteins indicates microtubule polarity in the *Drosophila* oocyte, epithelium, neuron and muscle. Development *124*, 461–470.

Cui, W. and Hawley, R. S. (2005). The HhH(2)/NDD Domain of the *Drosophila* Nod chromokinesin-like protein is required for binding to chromosomes in the oocyte nucleus. Genetics (*in press*).

Desai, A., and Mitchison, T. J. (1997). Microtubule polymerization dynamics. Annu. Rev. Cell Dev. Biol. *13*, 83–117.

Desai, A., Verma, S., Mitchison, T. J., and Walczak, C. E. (1999). Kin I kinesins are microtubule-destabilizing enzymes. Cell *96*(1), 69–78.

Dickinson, R. B., and Purich, D. L. (2002). Clamped-filament elongation model for actin-based motors. Biophys. J. *82*, 605–617.

Goshima, G. and Vale R. D. (2003). The roles of microtubule-based motor proteins in mitosis: comprehensive RNAi analysis in the *Drosophila* S2 cell line. J. Cell Biol. *162*(6),1003–1016.

Howard, J., and Hyman, A. A. (2003). Dynamics and mechanics of the microtubule plus end. Nature *422*(6933), 753–758.

Jauschke, J., Gervais, L., Kaltschmidt, J. A., Lopez-Schier H. Johnson, D. S., Brand, A. H., Roth, S., and Guichet, A. (2002). Polar transport in the *Drosophila* oocyte requires Dynein and Kinesin I cooperation. Curr. Biol. *12*, 1971–1981.

Li, M., McGrail, M., Serr, M., and Hays, T. S. (1994). *Drosophila* cytoplasmic dynein, a microtubule motor that is asymmetrically localized in the oocyte. J. Cell Biol. *126*(6),1475–1494.

Matthies, H. J., Baskin, R. J., and Hawley, R. S. (2001). Orphan kinesin NOD lacks motile properties but does possess a microtubule-stimulated ATPase activity. Mol. Biol. Cell *12*, 4000–4012.

Matthies, H. J., Messina, L. G., Namba, R., Greer, K. J., Walker, M. Y., and Hawley, R. S. (1999). Mutations in the *alpha-tubulin 67*C gene specifically impair achiasmate segregation in *Drosophila melanogaster*. J. Cell Biol. *147*, 1137–1144.

Rasooly, R. S., New, C. M., Zhang, P., Hawley, R. S., and Baker, B. S. (1991). The *lethal(1)TW-6$^{cs}$* mutation of *Drosophila melanogaster* is a dominant antimorphic allele of nod and is associated with a single base change in the putative ATP-binding domain. Genetics *129*, 409–422.

Rasooly, R. S., Zhang, P., Tibolla, A. K., and Hawley, R. S. (1994). A structure-function analysis of NOD, a kinesin-like protein from *Drosophila melanogaster*. Mol. Gen. Genet. *242*, 145–151.

Rice S. *et al.* (1999). A structural change in the kinesin motor protein that drives motility. Nature *402*(6763),778–784.

Rieder, C. L., Davison, E. A., Jensen, L. C., Cassimeris, L., and Salmon, E. D. (1986). Oscillatory movements of monooriented chromosomes and their position relative to the spindle pole result from the ejection properties of the aster and half-spindle. J. Cell Biol. *103*(2), 581–591.

Riparbelli, M. G. and Callaini, G. (2005). The meiotic spindle of the *Drosophila* oocyte: the role of Centrosomin and the central aster. J. Cell Sci. *118*, 2827–2836.

Rørth, P. (1998). Gal4 in the *Drosophila* female germline. Mech. Dev. *78*, 113–118.

Serbus, L. R., Cha, B. J., Theurkauf, W. E., and Saxton, W. M. (2005). Dynein and the actin cytoskeleton control kinesin-driven cytoplasmic streaming in *Drosophila* oocytes. Development. *132*(16):3743–3752.

Shiroguchi, K., Ohsugi, M., Edamatsu, M., Yamamoto, T., and Toyoshima, Y. Y. (2003). The second microtubule-binding site of monomeric kid enhances the microtubule affinity. J. Biol. Chem. *278*(25), 22460–22465.

Sproul, L. R., Anderson, D. J., Mackey, A. T., Saunders, W. S., and Gilbert, S. P. (2005). Cik1 targets the minus-end Kinesin depolymerase kar3 to microtubule plus ends. Curr. Biol. *15*(15), 1420–14277.

Theurkauf, W. E., and Hawley, R. S. (1992). Meiotic spindle assembly in *Drosophila* females: behavior of nonexchange chromosomes and the effects of mutations in the *nod* kinesin-like protein. J. Cell Biol. *116*, 1167–1180.

Van Doren, M., Williamson, A. L., and Lehmann, R. (1998). Regulation of zygotic gene expression in *Drosophila* primordial germ cells. Curr. Biol. *8*, 243–246.

Woehlke, G., Ruby, A. K., Hart, C. L., Ly, B., Hom-Booher, N., and Vale, R. D. (1997). Microtubule interaction site of the kinesin motor. Cell *90*, 207–216.

Zhang, P., Knowles, B. A., Goldstein, L.S.B., and Hawley, R. S. (1990). A kinesin-like protein required for distributive chromosome segregation in *Drosophila*. Cell *62*, 1053–1062.